Review

Development of cortical folding during evolution and ontogeny

Karl Zilles[1,2,3,4], Nicola Palomero-Gallagher[1,2], and Katrin Amunts[1,2,3]

[1] Research Centre Juelich, Institute for Neuroscience and Medicine (INM-1), Juelich, Germany
[2] Juelich–Aachen Research Alliance (JARA), Translational Brain Medicine, Juelich, Germany
[3] C. & O. Vogt Institute for Brain Research, University of Düsseldorf, Düsseldorf, Germany
[4] Rheinisch–Westfaelische Technische Hochschule (RWTH) Aachen University, Department of Psychiatry, Psychotherapy, and Psychosomatics, Aachen, Germany

Cortical folding is a hallmark of many, but not all, mammalian brains. The degree of folding increases with brain size across mammals, but at different scales between orders and families. In this review we summarize recent studies that have shed light on cortical folding and discuss new models that arise from these data. Genetic analyses argue for an independent development of brain volume and gyrification, but more recent data on the cellular development of the cortex and its connectivity highlight the role of these processes in cortical folding (grey matter hypothesis). This, and the widely discussed tension hypothesis, further tested by analyzing the mechanical properties of maturing nerve fibers, synapses, and dendrites, can provide the basis for a future integrative view on cortical folding.

Cortical folding: a morphological hallmark of many mammalian brains

Mammalian species have folded (i.e., gyrencephalic) or smooth (i.e., lissencephalic) cortical surfaces that can be characterized by their gyrification index (GI). The GI is a measure of the degree of folding and is the ratio between the total outer cortical surface (i.e., the superficially exposed portion plus the part buried in the sulci) and the superficially exposed part of the outer surface. GI measurements clearly show that the human brain is the largest and most intensively folded primate brain [1–4] (for various methods used to measure the GI see Box 1). However, quantitative data on the degree of folding of the larger brains of cetaceans [5,6], Artiodactyla [4], and elephants [7] demonstrate that these brains display even more gyrification than the human brain. Such comparisons seem to support the popular opinion that folding is a consequence of increasing brain size across mammalian orders (Figure 1), but they do not consider the substantial differences between orders in the structure and dimensions of gyri, sulcal patterns, the number and internal organization of cortical areas, as well as underlying connectivity and developmental processes during evolution and ontogeny.

Popular hypotheses explained cortical folding as a consequence of the restricted space in the skull ([8,9] for review of this and various other hypotheses) or, more recently, as an effect of the tension exerted by fiber tracts [10,11] that connect various cortical areas or the cortex with subcortical sources and targets. Other hypotheses emphasized the developmental mechanisms of the cortex [12] or the relation between the thicknesses of supragranular (i.e., cortical layers I–III) versus infragranular layers (i.e., cortical layers V–VI) as major causes for gyrification [13]. Given that the degree of gyrification varies widely among mammals and originates during fetal and early postnatal development, the developmental perspective can provide valuable information for understanding the driving forces behind cortical folding. The current review addresses the quantitative dimension of gyrification as a morphological hallmark of brain development. Furthermore, we propose that the mechanistic influence of fiber tracts and the intrinsic organization and ontogenetic development of the cerebral cortex are related, rather than alternative, processes that enable the progressive differentiation of the cortex during evolution and ontogeny.

GI: regional and intersubject variability, plasticity, and impairment by pathology

The GI of human brains is greatest in the prefrontal and parieto-occipito-temporal association regions, given their abundant cortico-cortical and callosal connections [1]. The GI (averaged over the whole cortex) shows considerable inter-subject variability and ranges between 2.21 and 2.97 (mean GI = 2.56 ± 0.02) in postmortem samples of 61 female and male brains (age range 16–91 years) [1]. In a different sample of 242 female and male brains (age range 19–85 years), a mean GI of 2.29 ± 0.08 was reported based on *in vivo* structural magnetic resonance imaging (MRI) [14] (Figure 1b). The GI differs significantly between left and right hemispheres in male but not in female brains in a postmortem sample [1]. In an *in vivo* sample of 96 male and 146 female brains [14] the GI was found to differ significantly between males and females. No significant correlations are found between the average GI of the total cortex, body weight and length, brain weight, or volume of the cortex [1,14]. In samples of 12 adult rhesus monkeys and 97 baboons (age range 7.3–27.3 years), the mean GIs of the total cortex (rhesus, 1.88 ± 0.08; baboon, 1.89 ± 0.15) do not correlate with age, sex, or brain weight [13–15]. In conclusion, cortical folding does not systematically vary with brain size within each of these primate species, but is

Corresponding author: Zilles, K. (k.zilles@fz-juelich.de)
Keywords: cerebral cortex; cortical folding; evolution; ontogeny; cortical development; tension hypothesis.

  http://dx.doi.org/10.1016/j.tins.2013.01.006

Box 1. How to measure cortical folding

Cortical folding is measured by a variety of different methods:

- Contour-based, 2D, manually traced or automated computational measurements in histological serial sections or MRI of the brain. The GI increases with an increasing degree of folding. It can be calculated as ratio averaged over the whole cortex or in defined regions of the cortex [1,2,4,13,41,44,73,74].
- Various surface-based and graph matching methods for the *in vivo* and postmortem analysis of the cortical folding averaged over the whole cortex or of its regionally specific degree of folding. The measurements rely on surface reconstructions (e.g., triangulated surfaces based on MRI brain data sets) [14,16,18,25,31,39,45,72,75–85].
- Various stereological approaches for measuring cortical surfaces in histological sections [5,86,87].
- A surface-based approach that relies in covering both the superficially exposed cortical surface and the part within the sulci with small pieces of paper or gold foil [7]. This approach provides valuable data, but the tedious and time-consuming procedure has been replaced by the methods described above.

correlated with brain size in inter-species comparisons (Figure 1b). The variability of the GI within a species indicates a brain size-independent plasticity at this level, which may be the consequence of individual variations in developmental processes, functional, or environmental challenges.

Global and regional-specific changes of GI have been reported in brains of healthy subjects [16]. For example, the depth of the central sulcus, and thus the local GI, increases with the duration and early onset of professional training as well as motor performance in keyboard players [17]. A correlation between gyrification and cognitive functions has also been discussed [18,19]. In meditation practitioners, a higher gyrification is found in the anterior insula, precentral and fusiform gyrus, and right precuneus when compared to controls [19]. Furthermore, positive correlations exist between the years of meditation and the increase in folding [20]. A significant age-related decline in the GI was recently reported in the prefrontal cortex of patients with mental disorders [21]. Changes in gyral complexity are described not only in malformations [22] but also in other pathologies. For instance, a decrease in gyrification occurs in epilepsy [23], attention deficit hyperactivity disorder [24], dementia [25], mental retardation [26] and dyslexia [27]. By contrast, a thinning of the cortex accompanied by an increase in gyrification is found in 22q11.2 deletion [28], Williams syndrome [29], autism [30], and schizophrenia [31,32]. These findings in normal and pathologically impaired brains suggest not only a relationship between the intensity of cortical folding and cerebral function and dysfunction, but also between the shape and localization of sulci as macroscopic landmarks and the segregation of the cortex into functional and cytoarchitectonic areas. A comprehensive discussion of these relationships, however, would exceed the framework of this review.

Evolution of cortical folding

Relation of brain size and GI across mammalian orders

Cetacea and elephants have the highest GI, followed by humans (Figure 1). The GI values for some non-human primates, Artiodactyla, Perissodactyla, and the seal (Figure 1a) reach the range for humans (Table 1, Figure 1b). The gyrification of the different Cetacea, including the low GI of the harbor porpoise (Figure 1a), is above the GIs of Artiodactyla. The average GI of rodents is even lower than that of carnivores, although the large-brained Patagonian mara and the capybara (Figure 1a) are included in the rodent sample.

Artiodactyla and Cetacea show a significant increase of GI with increasing brain size (Table 1). The slopes of the regressions, however, differ significantly between both orders, with the Cetacea having a faster increase in GI per unit increase brain size than Artiodactyla (Figure 1a). This difference between orders is also demonstrated using allometric scaling [4], although future studies at the level of families may reveal that even there a different scaling can be detected.

The ratio between the total outer contour of the cortex (along the pial surface) and the inner contour (along the cortex/white matter border) provides an interesting perspective on gyrification (different from that of the GI) in primates, carnivores, Perissodactyla, Artiodactyla, and rodents [4]. This ratio implicitly takes cortical thickness into account as a factor possibly influencing cortical folding. Comparing this ratio between four orders, the Artiodactyla have the lowest ratio, the rodents the highest, and carnivores and primates are found at intermediate positions. In other words, the thinner the average cortical thickness, the more intensive is the cortical folding. This conclusion is further supported by studies in Cetacea, which have the thinnest cortex and the highest GI of all mammals. The extremely folded cetacean cortex not only has fewer neurons and lower cell densities than that of primates with the same brain size, but also has a completely different cytoarchitecture with more prominent layers I and VI as well as a complete lack of layer IV [6,33,34]. This deviation from the Bauplan of the neocortex of most other mammalian orders indicates a different laminar organization [33] and, putatively, changes in the wiring of afferent and efferent fiber tracts. Thus, the gyrification of the cetacean cortex is based on different intra-cortical organization compared to primates. Consequently, 'cortical thickness' does not signify a homogeneous and comparable tissue property across mammalian orders, but can comprise largely different organizational types of the cerebral cortex. In conclusion, cortical folding of mammals increases with decreasing cortical thickness in an order-specific scaling [4]. Thinner cortices allow for smaller and more numerous gyri, which results in more intense cortical folding relative to brain weight.

The cortical thickness of different areas varies considerably within each species, as well as between species, families, and orders. In addition, the number of cortical areas increases, and their intrinsic architectonic organization and connectivity changes as a consequence of cortical evolution [11,35–37]. Thus, cortical thickness must be broken down into the underlying tissue properties. Consequently, a recent study suggests that the fraction of cortical neurons connected through the white matter and the average cross-sectional area of axons in the white matter, together with their mechanical properties, are important determinants of cortical folding [9]. Accordingly, the different degrees of

Table 1. Brain size and gyrification index (GI) in various mammalian orders, families, and species

Order	Family	Species	Common name	Brain (volume, weight)	GI[a]	Refs
Monotremata	Tachyglossidae	*Zaglossus bruijni*	Western long-beaked echidna	53	1.51	[7]
Didelphimorhia	Didelphidae	*Marmosa sp.*	Mouse opossum	1.24	1.01	[5]
		Didelphis virginiana	Opossum	4.25	1.11	[5]
Dasyuromorphia	Dasyuridae	*Sarcophilus harrisii*	Tasmanian devil	15	1.33	[7]
Diprotodontia	Macropodidae	*Wallabia rufogrisea*	Wallaby	25	1.23	[5]
		Macropus melanops	Kangaroo	39	1.41	[5]
	Phalangeridae	*Trichosurus vulpecula*	Common brushtail possum	12.5	1.23	[7]
Proboscidea	Elephantidae	*Loxodonta africana*	African elephant	4925	3.81	[7]
Rodentia	Castoridae	*Castor canadensis*	North American beaver	39	1.02	[4]
	Cricetidae	*Mesocricetus auratus*	Hamster	0.90	1.01	[4]
	Muridae	*Rattus norvegicus*	Rat	2.48	1.02	[4]
		Mus musculus	Mouse	0.65	1.03	[4]
	Caviidae	*Dolichotis patagonum*	Patagonian mara	29	1.42	[87]
		Hydrochaeris hydrochaeris	Capybara	51	1.30	[4]
	Dasyproctidae	*Dasyprocta leporina*	Agouti	17.2	1.23	[4]
Lagomorpha	Leporidae	*Oryctolagus cuniculus*	Rabbit	12	1.15	[87]
Carnivora	Canidae	*Vulpes vulpes*	Fox	45	2.01	[5]
				45	1.80	[87]
		Canis latrans	Coyote	85	1.80	[5]
	Ursidae	*Ursus arctos*	Brown bear	350	1.99	[7]
		Ursus maritimus	Polar bear	459	2.04	[4]
	Procyonidae	*Procyon lotor*	Raccoon	43	1.85	[5]
	Mustelidae	*Martes foina*	Beech marten	27	1.86	[7]
		Mustela putorius	Ferret	11	1.63	[7]
		Phoca sp.	Seal	187	2.82	[7]
	Felidae	*Felis domestica*	Cat	31	1.65	[7]
				30	1.60	[87]
				37	1.50	[4]
		Panthera leo	Lion	259	1.94	[7]
				258	1.85	[4]
	Hyaenidae	*Crocuta crocuta*	Hyena	163	1.74	[4]
	Herpestidae	*Cynictis penicillata*	Mierkat	15	1.35	[4]
Perissodactyla	Equidae	*Equus caballus*	Horse	590	1.99	[7]
				532	2.80	[87]
		Equus burchelii	Zebra	521	2.94	[4]
Artiodactyla	Camelidae	*Lama glama*	Llama	200	2.70	[4]
	Suidae	*Sus scrofa domestica*	Domestic pig	112	2.00	[7]
				180	2.18	[87]
				95	2.16	[4]
	Cervidae	*Odocoileus virginianus*	White-tailed deer	160	2.27	[4]
	Bovidae	*Bos taurus*	Domestic cattle	540	2.54	[7]
				441	2.49	[87]
		Bos taurus indicus	Zebu	474	2.53	[4]
		Ovis aries	Sheep	118	2.29	[7]
				140	1.94	[87]
		Capra aegagrus hircus	Domestic goat	105	1.81	[7]
Cetacea	Delphinidae	*Phocaena phocaena*	Harbor porpoise	455	3.00	[7]
		Pseudorca crassidens	False killer whale	3650	4.97	[5]
		Delphinus delphis	Baird's dolphin	722	3.99	[5]
		Tursiops truncatus	Atlantic bottlenose dolphin	1145	4.47	[5]
		Tursiops aduncus	Pacific bottlenose dolphin	1498	4.75	[5]
		Globicephala melas	Atlantic pilot whale	2580	5.03	[5]
		Globicephala macrorhynchus	Pacific pilot whale	2842	5.55	[5]
		Grampus griseus	Risso's dolphin	1500	4.25	[5]

[a]GI determinations employed histological images from Comparative Mammalian Brain Collections of the University of Wisconsin and Michigan State (contour-based measurement) in [4]; formalin-fixed brain, histology, calculated from stereological measurement in [5]; formalin-fixed postmortem, measurement by brain surface coverage with paper in [7]; formalin-fixed brain, histology, calculated from stereological measurement in [87].

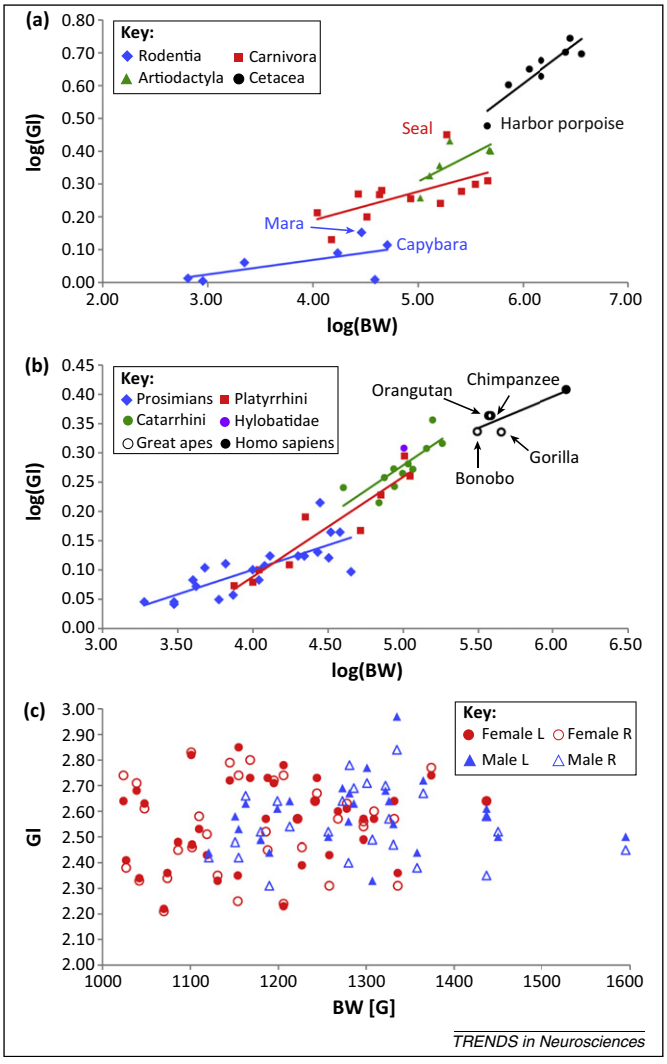

Figure 1. Relations between gyrification index (GI) and brain weight (BW) in mammalian species. **(a)** Allometric comparisons for Artiodactyla [log(GI) = 0.146log(BW) − 0.513; $R^2 = 0.465$, $P = 0.06$], Carnivora [log(GI) = 0.088log(BW) − 0.162; $R^2 = 0.393$, $P = 0.03$], Cetacea [log(GI) = 0.242log(BW) − 0.846; $R^2 = 0.815$, $P < 0.001$], and Rodentia [log(GI) = 0.044log(BW) − 0.108; $R^2 = 0.281$, $P = 0.13$]. The slopes of the regressions differ significantly between Artiodactyla and Cetacea (ANCOVA; $P < 0.001$). **(b)** Allometric comparisons in primates. Hominidae comprising *Homo sapiens, Pongo pygmaeus, Gorilla gorilla, Pan troglodytes,* and *Pan paniscus* [log(GI) = 0.106log(BW) − 0.245; $R^2 = 0.573$, $P = 0.03$], Catarrhini [log(GI) = 0.174log(BW) − 0.592; $R^2 = 0.573$, $P < 0.001$], Platyrrhini [log(GI) = 0.17log(BW) − 0.593; $R^2 = 0.895$, $P < 0.001$], and prosimians [log(GI) = 0.083log(BW) − 0.235; $R^2 = 0.605$, $P < 0.001$]. The slopes of the regressions differ significantly (ANCOVAs) between prosimians and Platyrrhini ($P = 0.006$), Catarrhini ($P < 0.001$) and Hominidae ($P < 0.001$). In panels (a) and (b) each point refers to a different species. **(c)** Relationship between GI and brain weight within the human brain. Each point refers to a male or a female individual and the GI of the left or right hemisphere. Data extracted from [1,2,4,5,13,14,87–89].

gyrification across mammals correspond to different combinations of these parameters.

In this context, comparing the relationship between GI and cortical thickness in the cerebral and cerebellar cortices provides a further insight. The cerebellar cortex is much more folded than the cerebral cortex, and the cerebellar folds, termed folia, are much thinner than the gyri of the cerebral cortex. The very high GI of the cerebellar cortex and the thinning of the folia are possible because the white matter of the cerebellar folia contains only fibers from and to extracerebellar brain regions and to cerebellar nuclei. Thus, the cerebellum lacks the huge amount of long- and short-range cortico-cortical connections [38] found between the gyri of the cerebral cortex. Consequently, the white matter between the cortical ribbons of the folia is relatively thinner than that of cortical gyri.

Relationship between brain size and GI within the primate order

The GI increases significantly with brain size within the primates order (Figure 2). As such, the GI of prosimians overlaps with those of new world monkeys, and the latter with those of old world monkeys (Figures 1b and 2). The small-brained prosimians show weakly folded to nearly unfolded cortical surfaces (Figure 3), and only the larger-brained (over 10 g) prosimians have moderately folded surfaces. When the GI of prosimians surpasses a value of 1.25 (Figure 2), the intraparietal sulcus becomes visible, indicating a considerable enlargement of the parietal association cortex between the somatosensory and visual cortices, and its subdivision into a superior and inferior parietal lobule (Figure 3). In new world monkeys, the intraparietal sulcus is regularly present and missing only in the small-brained common marmoset (Figure 3). The GI reaches higher values in catarrhines, and is maximal in human brains (Figures 1b and 2). The slopes of the allometric regressions differ significantly between prosimians and Platyrrhini, Catarrhini, and Hominidae. The trend describing GI with respect to brain weight has the steepest slope for Platyrrhini and Catarrhini, followed by the Hominidae, and finally the prosimians (Figure 1b). Notably, the increase in GI per volume increase in brain size is not significantly different between Hominidae and Cercopithecoidae. To our knowledge, the scaling of the GI described here is based on the largest number of different primate species ever compared (Figure 2).

A considerable regional difference in cortical folding with increasing brain size in primates has also been demonstrated (Figure 3). During ontogeny, folding appears first in the occipital, parietal, and superior temporal regions. Later, and together with the late increase in size of the prefrontal and inferior temporal cortex, folding increases in these regions. The GI averaged over the whole cerebral cortex should, therefore, be interpreted on the background of the heterochronous ontogenetic development of the various cortical regions, particularly with respect to the prefrontal cortex with its late evolving areas.

The heritability of brain size, brain surface area, and GI differs between primate species, and is much lower in humans than baboons [14]. Accordingly, only 30% of the intra-species phenotypic variance can be attributed to genetic variation among human subjects, but 71% among baboons. Furthermore, in both species it could be demonstrated by genetic correlation analysis, using the known pairwise kinship between members of a pedigree and the individual values for brain size and GI, that the same genetic changes increase brain volume and surface area, but decrease GI [14]. In normal brains of 180 adult baboons, the areas, lengths, and depths of various sulci showed a degree of heritability of around 40% [15], indicating a greater influence of environmental over genetic factors to the sulcal phenotype. In line with this, studies in mono- and dizygotic human twins without a history of

neurological or psychiatric illnesses support the view that the pattern and degree of gyrification are determined more by non-genetic than genetic factors [39,40], whereas brain size is more strongly controlled by genetic factors. All of these results highlight the fundamental difference between the brain size–GI relationship across species, families, or orders, in contrast to an analysis between individuals within the same species. They support the hypothesis of two independent sets of selective pressures that produce increases in brain size and GI [14].

To the best of our knowledge, comparable studies of the intra-species variability of brain size and GI are lacking in other mammalian species. Only one study in dogs of different breeds reports a significant correlation between brain size and GI [41]. However, different dog races show large differences in body size, shape of the cranium, and an

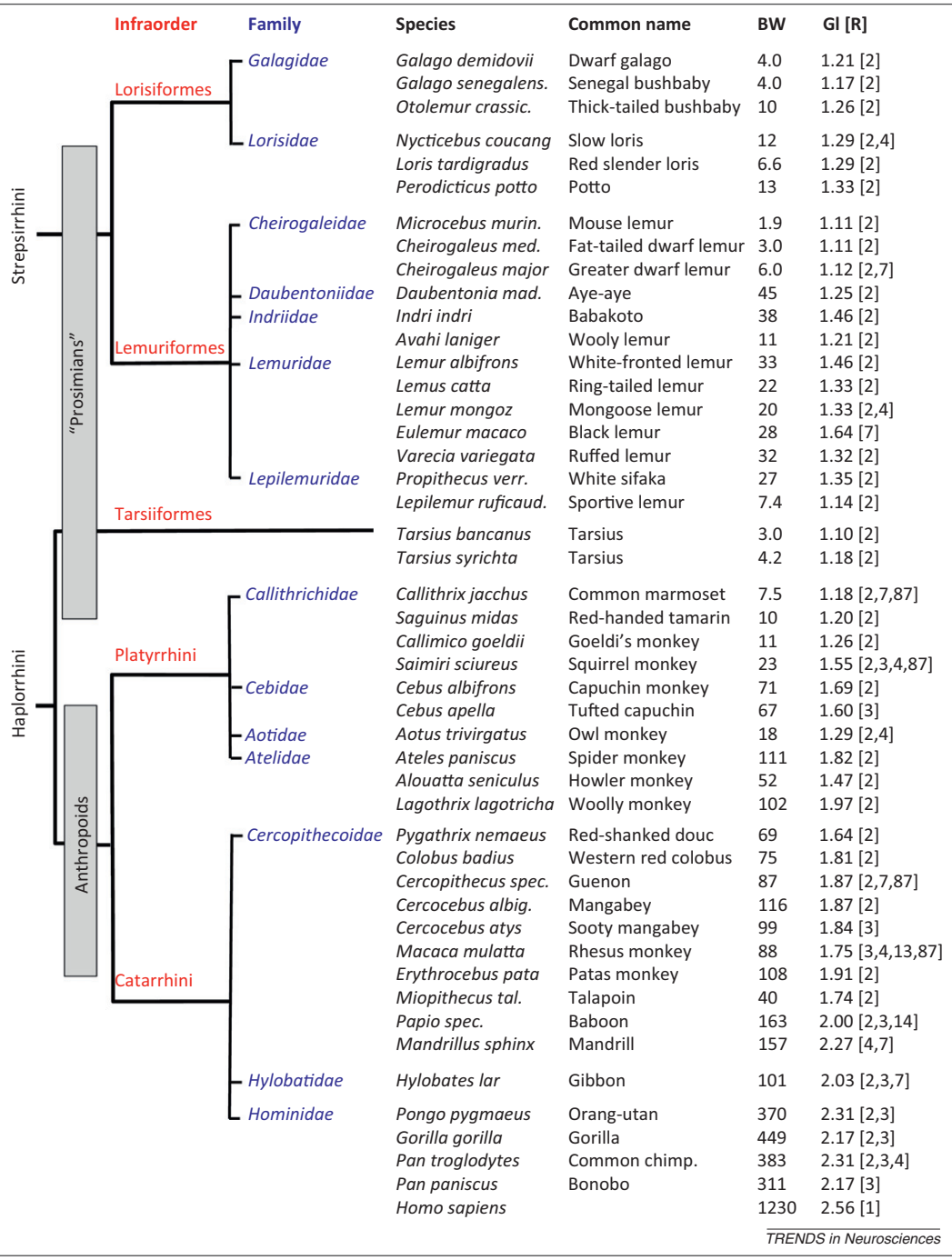

Figure 2. Mean gyrification indices and brain weights of primates. References to data sources including sample size and sex are given in square brackets. Formalin-fixed brains, histological sections from the Stephan Collection and Zilles Collection, Brain Research Institute, University Düsseldorf, Germany, contour-based measurement, adult animals [2]. *In vivo* MRI, contour-based measurement, adult and young animal; *Saimiri sciureus*, 3 males (M), 1 female (F); *Cebus apella*, 2 M, 2 F; *Cercocebus atys*, 2 M, 2 F; *Macaca mulatta*, 2 M, 2 F; *Papio cynocephalus*, 2 M; *Hylobates lar*, 2 M, 2 F; *Pongo pygmaeus*, 3 M, 1 F; *Gorilla gorilla*, 1 M, 1 F; *Pan troglodytes*, 3 M, 3 F; *Pan paniscus*, 2 M, 2 F [3]. Histological images from Comparative Mammalian Brain Collections of the University of Wisconsin, and Michigan State, contour-based measurement [4]. Formalin-fixed postmortem, measurement by brain surface coverage with paper [7]. *Macaca mulatta*, formalin-fixed brains, histology, contour-based measurement, 12 adult animals [13]. *Papio hamadryas, in vivo* MRI, surface-based measurement, 46 males, 51 F, age range 7–27 years [14]. Single formalin-fixed brains, histology; calculated from stereological measurement [87]. GI, gyrification index; R, reference.

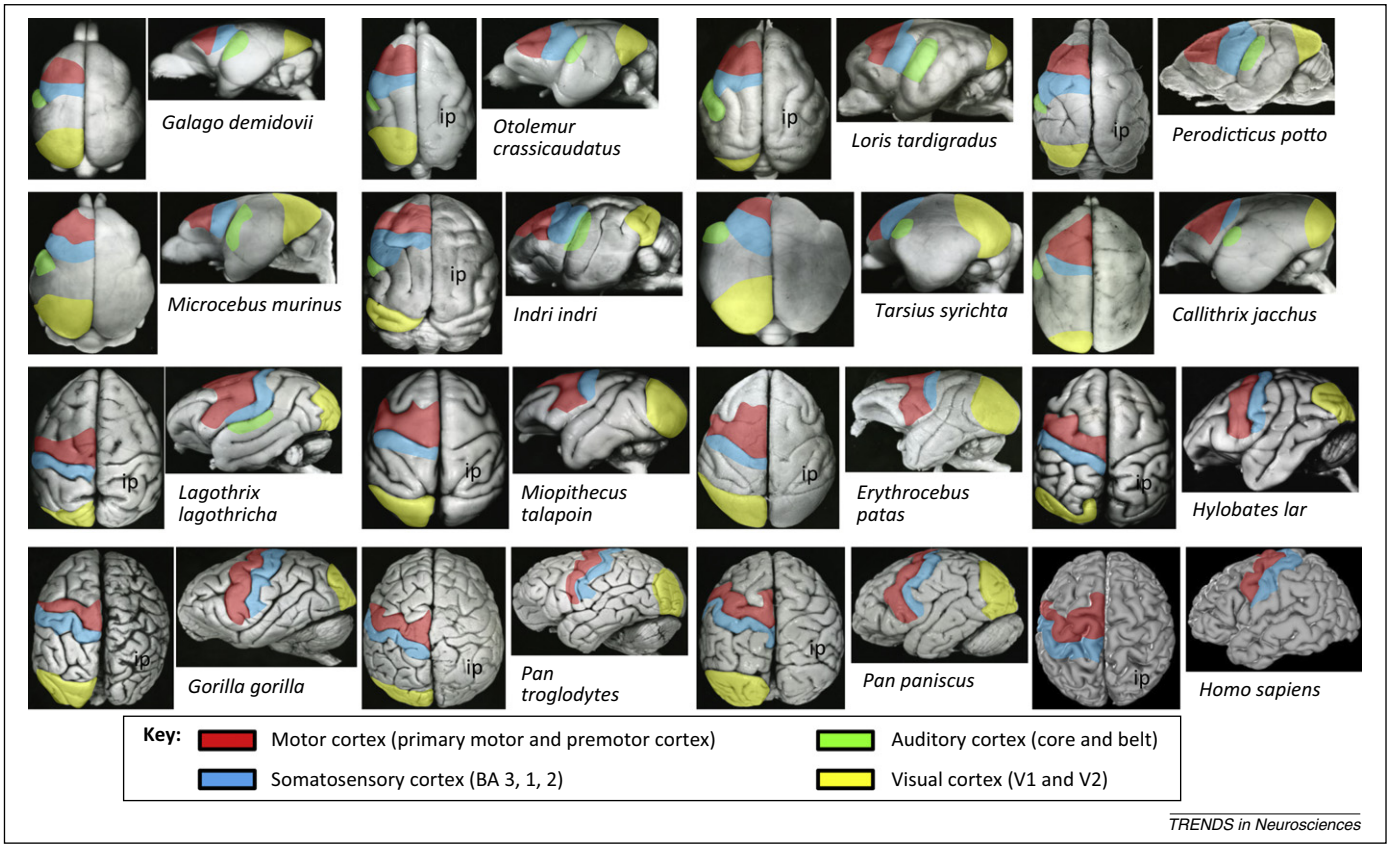

Figure 3. Variability of cortical folding in different primate species. Dorsal (left columns) and lateral (right columns) views of primate brains. Approximate position and size of motor, somatosensory, auditory, and visual areas are labeled based on published brain maps [90–95]. Brain images: Stephan Collection, C. & O. Vogt Institute of Brain Research, University of Düsseldorf and the JuBrain website (https://jubrain.fz-juelich.de/); ip, intraparietal sulcus.

exceptionally high 2.4-fold variation of brain size, when compared to data for human (1.1-fold [14] and 1.6-fold [2]), rhesus (1.3-fold [13]), and baboon (1.1-fold [14]). The GI varies only by 1.19-fold in different dogs (i.e., much less than brain size varies), which further supports the assumption of different control mechanisms for brain size and folding.

In summary, although the GI correlates positively with brain size and cortical surface across mammalian orders, this relationship is not found within a species.

Ontogeny of the GI

In macaque monkeys, mean GI remains low up to fetal day 90, increases drastically from day 100, and reaches adult value by fetal day 150 (birth date 166 ± 8) [42,43]. Cortical folding of the human brain starts around the 16th week of gestation, increases rapidly during the first trimester, and reaches a transient maximum between weeks 66 and 80 postconception [44]. From this time on, the GI declines by 18% from a maximal value of 3.03 to the adult level, which is reached at an age of almost 23 years [44] (Figure 4a). An MRI study confirms this folding overshoot [45]. The mechanisms underlying this developmental course are not sufficiently understood, but it may be speculated that perinatal pruning with programmed cell death and reduction of cell numbers and connectivity may lead to the GI reduction [46]. However, the decrease in GI continues into adulthood, whereas the perinatal overshooting of synaptic density seems to reach a plateau much earlier than the GI [47].

Alternatively, the reduction of GI can be explained by an increasing gyral width driven by the peak of myelination of input and output fibers during the postnatal period. The GI will decrease if the sulcal depths remain constant or start to decline [48,49]. Furthermore, the white matter continues to grow until the beginning of the third decade [50]. Thus, the postnatal maturation of nerve fibers and connectivity may explain the developmental course of cortical folding.

GI increases with increasing brain size up to a brain weight of approximately 530 g [44], but from this point a 2.5-fold enlargement of brain weight follows without any further increase in GI. The increase in brain weight is mainly driven by a twofold increase in the white matter volume [50], supporting the hypothesis of a causal relation between connectivity and GI. Apparently, folding and increase in brain weight are not controlled by identical developmental mechanisms.

Cortical folding during fetal and early postnatal development is also an important early marker of latter neurobehavioral development. *In vivo* imaging of premature newborns shows a delayed but balanced development of gyrification and surface in twins compared to singletons [51]. By contrast, newborns with intrauterine growth restrictions have a greater reduction in surface area than in folding [51]. The effect of the increasing brain weight on cortical volume is largely driven by the increase in cortical surface area, not cortical thickness [52]. The extent of cortical surface is probably determined by the number of

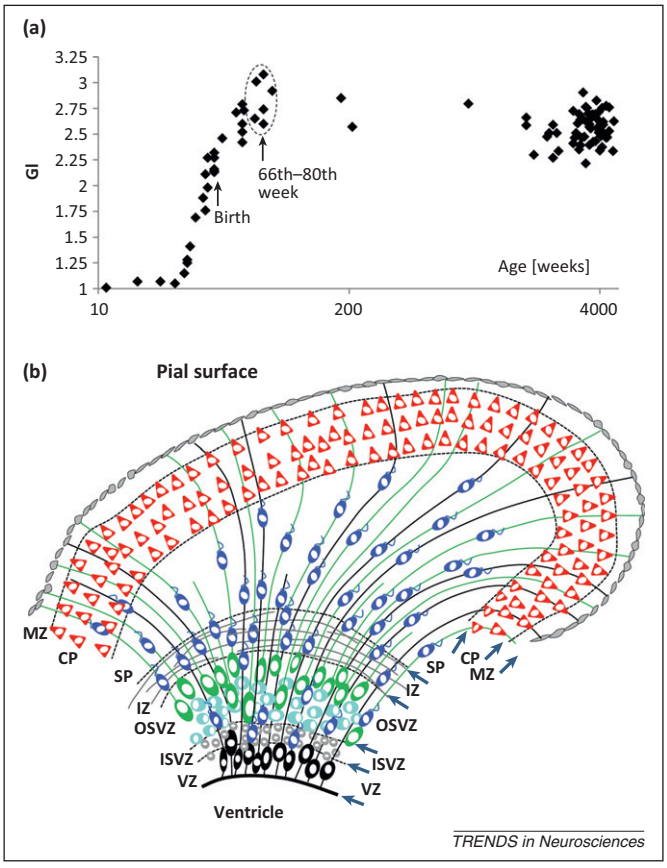

Figure 4. Ontogenetic development of cortical folding in humans. **(a)** Development of GI from fetal to adult stages. Age in weeks post-conception (birth 40th week). Data from [1,44]. **(b)** Development of the fetal hemispheric wall based on recent data [12,56,57,59,60,96]. Black, classical bipolar radial glia cells (vRG) in the ventricular zone (VZ); green, unipolar radial glia cells (oRG) in the outer subventricular zone (OSVZ); blue, immature neurons migrating along vRG and oRG cells to the cortical plate (CP); grey, intermediate progenitor cells in the inner subventricular zone (ISVZ); turquoise, progenitor cells and immature neurons in OSVC; red, young neurons in CP; IZ, intermediate zone with the first arriving nerve fibers establishing connection with immature neurons; MZ, marginal zone; SP, subplate.

cortical columns and neurons, and the growth of dendrites as well as input and output fibers, including their myelination. Therefore, cortical folding is probably caused by the synergistic effect of cell generation processes specific for gyrencephalic species as well as the evolving connectivity and mechanical properties of the fiber tracts and their constituents during pre- and postnatal development (discussed below).

Driving forces behind cortical folding

Previous reports [35,36] do not support the assumption of a simple relationship between gyrification and the total number of cortical neurons, or cortical volume or thickness, but underline the importance of the cortical column [53] as the essential building block. Thus, cell generation and migration as developmental processes leading to cortical columns seem to be important for understanding the driving forces behind cortical folding.

The differential growth of cortical layers is also proposed as a driving force of gyrification [54]. The model predicts folding when the growth of the supragranular layers exceeds that of the infragranular layers. Although studies of tissue compartments improved our understanding of the species-specificity of cortical organization [53], the regionally different proportions between supra- and infragranular layers have not been comprehensively studied and precisely related to regions of high or low GIs, although these compartments differ by their mechanical properties.

The two most widely discussed hypotheses are that folding is caused by: (i) growth processes during cortical development (grey matter hypothesis), and/or (ii) mechanical tension in axons (mechanical tension hypothesis). Both hypotheses will be discussed in the following sections.

Grey matter hypothesis

The subventricular zone of the fetal hemisphere (see [55] for the revised subdivision scheme of the hemispheric wall in primates) is subdivided into an inner (ISVZ) and outer (OSVZ) subventricular zone (Figure 4b) in human and monkey brains, and in brains of other gyrencephalic mammals, such as ferrets (Table 1) [56,57]. The lissencephalic brains of rats and mice do not develop a comparably broad and differentiated subventricular zone. The OSVZ is a proliferative region outside the ventricular zone that contains a lineage of neural stem and transit-amplifying intermediate progenitor cells [12,56,58–60] and expands considerably between gestational weeks 11 and 16 in humans [60], immediately before the onset of cortical folding. Transgenic mice expressing a stabilized version of β-catenin in neural precursor cells develop an increased cortical surface area and gyrification [61]. Thus, the OSVZ could play a key role in the tangential expansion and folding of the cerebral cortex, and it becomes the predominant proliferative zone in the developing human brain. The OSVZ modifies the trajectory of the migrating immature neurons by a recently discovered cell type, the unipolar intermediate radial glia cell (IRGC), which is a self-amplifying progenitor cell that generates a radially oriented scaffold in addition to the scaffold formed by the classical bipolar radial glia cells (vRG) [57,62,63]. In contrast to the latter cell type, most of the intermediate radial glia cells (oRG in Figure 4b) contact the pial, not the ventricular, surface. Notably, IRGC-like cells are also present in lissencephalic mammalian brains, although they are only found during late stages of cortical neurogenesis, are sparsely distributed, and do not constitute a distinct germinal layer [62,63]. The scaffold provided by the IRGCs resembles a fan, and the neurons migrating along this scaffold considerably increase the cortical surface. If the proliferation in the OSVZ is experimentally reduced, the cortical surface area and the cortical folding are also reduced [57]. Thus, the proliferation of IRGCs could be a driving force for the early tangential expansion of the fetal cortex and its folding [12,57,64,65].

The subplate zone (SP) plays a further important role in gyrification (Figure 4b), a role that was first described [66] in gyrencephalic mammalian brains. It is characterized by a slow and long-lasting developmental period [67,68]. SP has its largest dimension subjacent to late maturing and folding association cortices. It contains transient cortico-cortical and callosal connections before they enter the cortical plate (CP, Figure 4b). The protracted development and the dimension of the SP can explain the regional

heterochronicity of cortical folding [44] and the numerous, mainly smaller-sized gyri in the multimodal association regions, as well as the early interaction between cell proliferation and migration and the influence of fiber tension on folding. SP seems to be the structure that links the mechanisms behind the cellular proliferation and mechanical tension hypotheses.

Tension-based hypothesis

Tension above or below certain thresholds stimulates axonal elongation or retraction, respectively [69]. This finding is the cellular basis of a widely discussed and accepted tension-based hypothesis [10,11]. Because axons build the fiber tracts, gyrification can be explained by connectivity, more specifically by the 3D courses and the viscoelastic properties of fiber tracts. The first connections between cortical and other cortical and subcortical regions are visible during subplate development, and are maintained during migration and in the mature cortex via synapses that provide high adhesiveness of pre- to postsynaptic structures. There are many more tangentially organized (relative to the cortical surface) cortico-cortical than radially organized cortico-subcortical connections in the human forebrain. Consequently, the original tension hypothesis predicted an outward folding caused by strong cortico-cortical and weak cortico-subcortical connections, and an inward folding caused by an inverse relationship [10]. Moreover, folding makes the path between different interconnected cortical sites as short as possible. This is of advantage because the time for signal transmission is minimized within the organizational framework of the connectome.

A previous study demonstrated that axons are under considerable tension in the developing ferret brain [70]. However, a causal role of axonal tension for cortical folding by interpreting microdissection experiments in slices of ferret cortex and white matter during different developmental stages was not observed. Tension is found in radially as well as tangentially arranged axons in white matter tracts below gyri and sulci, and in radially arranged axons in gyri. Contrary to the original tension hypothesis [10], tension is not found across developing gyri [70]. Thus, tension cannot pull on the opposite walls of a gyrus and does not lead to an outward folding during initiation, nor when sustaining and maintaining folds. Despite this result, regional variations in tension may influence the region-specific shape of folding patterns and its correlation with the spatial organization of the connectome [71,72]. Using computational modeling, it was demonstrated that differential growth of cortical sites drives folding consistent with folding geometry and stress distribution [70]. In this model, a sulcus appears if a slowly growing cortical site first constrains the deformation of a neighboring faster growing site, and then the growth rates are switched for the generation of a second gyrus (intercortical 'phased' growth, [70]).

Future directions

It has been shown that cortical folding and brain size are correlated across species in order-specific scalings. The degree of folding is also related to the total number of neurons and their connections. Furthermore, gyrification is more influenced by non-genetic than genetic factors, whereas brain size is more strongly controlled by genetic factors. Further studies of the mechanisms of cortical development are necessary to understand the different scaling of brain size and gyrification between different orders as opposed to the variation between both measures within a species. To understand the evolution of gyrification, further comparative anatomical studies exploiting comprehensively stereological and genetic analyses in a variety of species and orders will be necessary. These species and orders should be chosen based on hypotheses on brain evolution, and not determined by the random effect of availability. To understand the causal mechanisms of gyrification, the grey matter hypothesis and the mechanical tension hypothesis should not be pursued as alternatives, but as complementary concepts. Cell proliferation and migration largely precedes the maturation of the connectivity, but there is a developmental window in which both processes overlap. Future research on the cortical and connectional development will be important for establishing an integrative theory of gyrification. Modeling and simulation approaches to cortical development will be necessary to understand the complex interactions of cellular biology and mechanical properties as well as their implementation in the four dimensions of brain space and development over time.

Acknowledgments

This work was supported partly by a National Institutes of Health grant (R01 MH092311-01) and a portfolio grant of the Helmholtz Association, Germany (HGF).

References

1 Zilles, K. *et al.* (1988) The human pattern of gyrification in the cerebral cortex. *Anat. Embryol.* 179, 173–179
2 Zilles, K. *et al.* (1989) Gyrification in the cerebral cortex of primates. *Brain Behav. Evol.* 34, 143–150
3 Rilling, J.K. and Insel, T.R. (1999) The primate neocortex in comparative perspective using magnetic resonance imaging. *J. Hum. Evol.* 37, 191–223
4 Pillay, P. and Manger, P.R. (2007) Order-specific quantitative patterns of cortical gyrification. *Eur. J. Neurosci.* 25, 2705–2712
5 Elias, H. and Schwartz, D. (1969) Surface areas of the cerebral cortex of mammals determined by stereological methods. *Science* 166, 111–113
6 Marino, L. *et al.* (2007) Cetaceans have complex brains for complex cognition. *PLoS Biol.* 5, e139
7 Brodmann, K. (1913) Neue Forschungsergebnisse der Grosshirnrindenanatomie mit besonderer Berücksichtigung anthropologischer Fragen. In *Verhandlungen der Gesellschaft Deutscher Naturforscher und Ärzte* (Witting, A., ed.), pp. 200–240, Vogel
8 Welker, W. (1990) Why does cerebral cortex fissure and fold? A review of determinants of gyri and sulci. In *Comparative Structure and Evolution of Cerebral Cortex* (Jones, E.G. and Peters, A., eds), pp. 3–136, Plenum Press
9 Mota, B. and Herculano-Houzel, S. (2012) How the cortex gets its folds: an inside-out, connectivity-driven model for the scaling of mammalian cortical folding. *Front. Neuroanat.* 6, 3
10 van Essen, D.C. (1997) A tension-based theory of morphogenesis and compact wiring in the central nervous system. *Nature* 385, 313–318
11 van Essen, D.C. (2007) Cerebral cortical folding patterns in primates: why they vary and what they signify. In *Evolution of Nervous Systems* (Kaas, J.H., ed.), pp. 267–276, Elsevier
12 Kriegstein, A. *et al.* (2006) Patterns of neural stem and progenitor cell division may underlie evolutionary cortical expansion. *Nat. Rev. Neurosci.* 7, 883–890

13 Armstrong, E. *et al.* (1991) Cortical gyrification in the rhesus monkey: a test of the mechanical folding hypothesis. *Cereb. Cortex* 1, 426–432
14 Rogers, J. *et al.* (2010) On the genetic architecture of cortical folding and brain volume in primates. *Neuroimage* 53, 1103–1108
15 Kochunov, P. *et al.* (2010) Genetics of primary cerebral gyrification: heritability of length, depth and area of primary sulci in an extended pedigree of Papio baboons. *Neuroimage* 53, 1126–1134
16 Hogstrom, L.J. *et al.* (2012) The structure of the cerebral cortex across adult life: age-related patterns of surface area, thickness, and gyrification. *Cereb. Cortex* http://dx.doi.org/10.1093/cercor/bhs231
17 Amunts, K. *et al.* (1997) Motor cortex and hand motor skills: structural compliance in the human brain. *Hum. Brain Mapp.* 5, 206–215
18 Fornito, A. *et al.* (2008) Variability of the paracingulate sulcus and morphometry of the medial frontal cortex: associations with cortical thickness, surface area, volume, and sulcal depth. *Hum. Brain Mapp.* 29, 222–236
19 Luders, E. *et al.* (2008) Mapping the relationship between cortical convolution and intelligence: effects of gender. *Cereb. Cortex* 18, 2019–2026
20 Luders, E. *et al.* (2012) The unique brain anatomy of meditation practitioners: alterations in cortical gyrification. *Front. Hum. Neurosci.* 6, 34
21 Bonnici, H.M. *et al.* (2007) Pre-frontal lobe gyrification index in schizophrenia, mental retardation and comorbid groups: an automated study. *Neuroimage* 35, 648–654
22 Francis, F. *et al.* (2006) Human disorders of cortical development: from past to present. *Eur. J. Neurosci.* 23, 877–893
23 Lin, J.J. *et al.* (2007) Reduced neocortical thickness and complexity mapped in mesial temporal lobe epilepsy with hippocampal sclerosis. *Cereb. Cortex* 17, 2007–2018
24 Wolosin, S.M. *et al.* (2009) Abnormal cerebral cortex structure in children with ADHD. *Hum. Brain Mapp.* 30, 175–184
25 Lebed, E. *et al.* (2012) Novel surface-smoothing based local gyrication index. *IEEE Trans. Med. Imaging* http://dx.doi.org/10.1109/TMI.2012.2230640
26 Zhang, Y. *et al.* (2010) Reduced cortical folding in mental retardation. *AJNR Am. J. Neuroradiol.* 31, 1063–1067
27 Casanova, M.F. *et al.* (2004) Reduced brain size and gyrification in the brains of dyslexic patients. *J. Child Neurol.* 19, 275–281
28 Bearden, C.E. *et al.* (2009) Alterations in midline cortical thickness and gyrification patterns mapped in children with 22q11.2 deletions. *Cereb. Cortex* 19, 115–126
29 Gaser, C. *et al.* (2006) Increased local gyrification mapped in Williams syndrome. *Neuroimage* 33, 46–54
30 Jou, R.J. *et al.* (2010) Cortical gyrification in autistic and Asperger disorders: a preliminary magnetic resonance imaging study. *J. Child Neurol.* 25, 1462–1467
31 Palaniyappan, L. and Liddle, P.F. (2012) Aberrant cortical gyrification in schizophrenia: a surface-based morphometry study. *J. Psychiatry Neurosci.* 37, 399–406
32 Schultz, C.C. *et al.* (2013) The visual cortex in schizophrenia: alterations of gyrification rather than cortical thickness – a combined cortical shape analysis. *Brain Struct. Funct.* 218, 51–58
33 Hof, P.R. and Van der Gucht, E. (2007) Structure of the cerebral cortex of the humpback whale, *Megaptera novaeangliae* (Cetacea, Mysticeti, Balaenopteridae). *Anat. Rec. (Hoboken)* 290, 1–31
34 Hof, P.R. *et al.* (2005) Cortical complexity in cetacean brains. *Anat. Rec. A: Discov. Mol. Cell. Evol. Biol.* 287, 1142–1152
35 Herculano-Houzel, S. (2011) Not all brains are made the same: new views on brain scaling in evolution. *Brain Behav. Evol.* 78, 22–36
36 Herculano-Houzel, S. *et al.* (2008) The basic nonuniformity of the cerebral cortex. *Proc. Natl. Acad. Sci. U.S.A.* 105, 12593–12598
37 Smaers, J.B. *et al.* (2010) Frontal white matter volume is associated with brain enlargement and higher structural connectivity in anthropoid primates. *PLoS ONE* 5, e9123
38 Sultan, F. (2002) Analysis of mammalian brain architecture. *Nature* 415, 133–134
39 Bartley, A.J. *et al.* (1997) Genetic variability of human brain size and cortical gyral patterns. *Brain* 120, 257–269
40 Hasan, A. *et al.* (2011) Prefrontal cortex gyrification index in twins: an MRI study. *Eur. Arch. Psychiatry Clin. Neurosci.* 261, 459–465
41 Wosinski, M. *et al.* (1996) Quantitative analysis of gyrification of cerebral cortex in dogs. *Neurobiology (Bp)* 4, 441–468
42 Sawada, K. *et al.* (2012) Fetal gyrification in cynomolgus monkeys: a concept of developmental stages of gyrification. *Anat. Rec. (Hoboken)* 295, 1065–1074
43 Sawada, K. *et al.* (2010) Ontogenetic pattern of gyrification in fetuses of cynomolgus monkeys. *Neuroscience* 167, 735–740
44 Armstrong, E. *et al.* (1995) The ontogeny of human gyrification. *Cereb. Cortex* 5, 56–63
45 Pienaar, R. *et al.* (2008) A methodology for analyzing curvature in the developing brain from preterm to adult. *Int. J. Imaging Syst. Technol.* 18, 42–68
46 Haydar, T.F. *et al.* (1999) The role of cell death in regulating the size and shape of the mammalian forebrain. *Cereb. Cortex* 9, 621–626
47 Huttenlocher, P.R. and Dabholkar, A.S. (1997) Regional differences in synaptogenesis in human cerebral cortex. *J. Comp. Neurol.* 387, 167–178
48 Magnotta, V.A. *et al.* (1999) Quantitative *in vivo* measurement of gyrification in the human brain: changes associated with aging. *Cereb. Cortex* 9, 151–160
49 Kochunov, P. *et al.* (2005) Age-related morphology trends of cortical sulci. *Hum. Brain Mapp.* 26, 210–220
50 Paus, T. *et al.* (2001) Maturation of white matter in the human brain: a review of magnetic resonance studies. *Brain Res. Bull.* 54, 255–266
51 Dubois, J. *et al.* (2008) Primary cortical folding in the human newborn: an early marker of later functional development. *Brain* 131, 2028–2041
52 Raznahan, A. *et al.* (2012) Prenatal growth in humans and postnatal brain maturation into late adolescence. *Proc. Natl. Acad. Sci. U.S.A.* 109, 11366–11371
53 DeFelipe, J. (2011) The evolution of the brain, the human nature of cortical circuits, and intellectual creativity. *Front. Neuroanat.* 5, 29
54 Richman, D.P. *et al.* (1975) Mechanical model of brain convolutional development. *Science* 189, 18–21
55 Bystron, I. *et al.* (2008) Development of the human cerebral cortex: Boulder Committee revisited. *Nat. Rev. Neurosci.* 9, 110–122
56 Fietz, S.A. *et al.* (2010) OSVZ progenitors of human and ferret neocortex are epithelial-like and expand by integrin signaling. *Nat. Neurosci.* 13, 690–699
57 Reillo, I. *et al.* (2011) A role for intermediate radial glia in the tangential expansion of the mammalian cerebral cortex. *Cereb. Cortex* 21, 1674–1694
58 Rakic, P. (1995) A small step for the cell, a giant leap for mankind: a hypothesis of neocortical expansion during evolution. *Trends Neurosci.* 18, 383–388
59 Hansen, D.V. *et al.* (2010) Neurogenic radial glia in the outer subventricular zone of human neocortex. *Nature* 464, 554–561
60 Lui, J.H. *et al.* (2011) Development and evolution of the human neocortex. *Cell* 146, 18–36
61 Chenn, A. and Walsh, C.A. (2002) Regulation of cerebral cortical size by control of cell cycle exit in neural precursors. *Science* 297, 365–369
62 Martinez-Cerdeño, V. *et al.* (2012) Comparative analysis of the subventricular zone in rat, ferret and macaque: evidence for an outer subventricular zone in rodents. *PLoS ONE* 7, e30178
63 Wang, X. *et al.* (2011) A new subtype of progenitor cell in the mouse embryonic neocortex. *Nat. Neurosci.* 14, 555–561
64 Molnár, Z. and Clowry, G. (2012) Cerebral cortical development in rodents and primates. *Prog. Brain Res.* 195, 45–70
65 Reillo, I. and Borrell, V. (2012) Germinal zones in the developing cerebral cortex of ferret: ontogeny, cell cycle kinetics, and diversity of progenitors. *Cereb. Cortex* 22, 2039–2054
66 Kostovic, I. and Rakic, P. (1990) Developmental history of the transient subplate zone in the visual and somatosensory cortex of the macaque monkey and human brain. *J. Comp. Neurol.* 297, 441–470
67 Judaš, M. *et al.* (2010) Populations of subplate and interstitial neurons in fetal and adult human telencephalon. *J. Anat.* 217, 381–399
68 Kostovic, I. and Judas, M. (2010) The development of the subplate and thalamocortical connections in the human foetal brain. *Acta Paediatr.* 99, 1119–1127
69 Dennerll, T.J. *et al.* (1989) The cytomechanics of axonal elongation and retraction. *J. Cell Biol.* 109, 3073–3083
70 Xu, G. *et al.* (2010) Axons pull on the brain, but tension does not drive cortical folding. *J. Biomech. Eng.* 132, 071013
71 Hilgetag, C.C. and Barbas, H. (2006) Role of mechanical factors in the morphology of the primate cerebral cortex. *PLoS Comput. Biol.* 2, e22

72 Toro, R. *et al.* (2008) Brain size and folding of the human cerebral cortex. *Cereb. Cortex* 18, 2352–2357
73 Moorhead, T.W. *et al.* (2006) Automated computation of the Gyrification Index in prefrontal lobes: methods and comparison with manual implementation. *Neuroimage* 31, 1560–1566
74 Dehay, C. *et al.* (1996) Contribution of thalamic input to the specification of cytoarchitectonic cortical fields in the primate: effects of bilateral enucleation in the fetal monkey on the boundaries, dimensions, and gyrification of striate and extrastriate cortex. *J. Comp. Neurol.* 367, 70–89
75 Paus, T. *et al.* (1996) Human cingulate and paracingulate sulci: pattern, variability, asymmetry, and probabilistic map. *Cereb. Cortex* 6, 207–214
76 Thompson, P.M. *et al.* (1996) Three-dimensional statistical analysis of sulcal variability in the human brain. *J. Neurosci.* 16, 4261–4274
77 Kennedy, D.N. *et al.* (1998) Gyri of the human neocortex: an MRI-based analysis of volume and variance. *Cereb. Cortex* 8, 372–384
78 Rivière, D. *et al.* (2002) Automatic recognition of cortical sulci of the human brain using a congregation of neural networks. *Med. Image Anal.* 6, 77–92
79 Cachia, A. *et al.* (2003) A primal sketch of the cortex mean curvature: a morphogenesis based approach to study the variability of the folding patterns. *IEEE Trans. Med. Imaging* 22, 754–765
80 Mangin, J.F. *et al.* (2004) A framework to study the cortical folding patterns. *Neuroimage* 23 (Suppl. 1), S129–S138
81 Régis, J. *et al.* (2005) 'Sulcal root' generic model: a hypothesis to overcome the variability of the human cortex folding patterns. *Neurol. Med. Chir. (Tokyo)* 45, 1–17
82 Mietchen, D. and Gaser, C. (2009) Computational morphometry for detecting changes in brain structure due to development, aging, learning, disease and evolution. *Front. Neuroinform.* 3, 25
83 Hill, J. *et al.* (2010) A surface-based analysis of hemispheric asymmetries and folding of cerebral cortex in term-born human infants. *J. Neurosci.* 30, 2268–2276
84 Li, K. *et al.* (2010) Gyral folding pattern analysis via surface profiling. *Neuroimage* 52, 1202–1214
85 Schaer, M. *et al.* (2012) How to measure cortical folding from MR images: a step-by-step tutorial to compute local gyrification index. *J. Vis. Exp.* 2, e3417
86 Schlenska, G. (1969) Messungen der Oberfläche und der Volumenanteile des Gehirns menschlicher Erwachsener mit neuen Methoden. *Z. Anat. Entwicklungsgesch* 128, 47–59
87 Schlenska, G. (1974) Volumen- und Oberflächenmessungen an Gehirnen verschiedener Säugetiere im Vergleich zu einem errechneten Modell. *J. Hirnforsch.* 15, 401–408
88 Frahm, H.D. *et al.* (1982) Comparison of brain structure volumes in Insectivora and Primates. I. Neocortex. *J. Hirnforsch.* 23, 375–389
89 Gebhard, R. *et al.* (1993) Gross anatomy and gyrification of the occipital cortex in human and non-human primates. In *Functional organisation of the human visual cortex* (Gulyás, B. *et al.*, eds), pp. 101–109, Pergamon Press
90 Brodmann, K. (1909) *Vergleichende Lokalisationslehre der Grosshirnrinde in ihren Prinzipien dargestellt auf Grund des Zellbaues*, Barth
91 Collins, C.E. *et al.* (2005) Overview of the visual system of Tarsius. *Anat. Rec. A: Discov. Mol. Cell. Evol. Biol.* 287, 1013–1025
92 Wong, P. *et al.* (2010) Overview of sensory systems of Tarsius. *Int. J. Primatol.* 31, 1002–1031
93 Wong, P. and Kaas, J.H. (2010) Architectonic subdivisions of neocortex in the Galago (*Otolemur garnetti*). *Anat. Rec. (Hoboken)* 293, 1033–1069
94 Zilles, K. *et al.* (1979) A quantitative approach to cytoarchitectonics. IV. The areal pattern of the cortex of *Galago demidovii* (E. Geoffroy, 1796) (Lorisidae, Primates). *Anat. Embryol.* 157, 81–103
95 Zilles, K. *et al.* (1979) A quantitative approach to cytoarchitectonics. V. The areal pattern of the cortex of *Microcebus murinus* (E. Geoffroy, 1828) (Lemuridae, Primates). *Anat. Embryol.* 157, 269–289
96 Rakic, P. (2009) Evolution of the neocortex: a perspective from developmental biology. *Nat. Rev. Neurosci.* 10, 724–735